

## Article

# Suzuki–Miyaura Catalyst-Transfer Polycondensation of Triolborate-Type Carbazole Monomers

Saburo Kobayashi <sup>1</sup>, Mayoh Ashiya <sup>1</sup>, Takuya Yamamoto <sup>2</sup>, Kenji Tajima <sup>2</sup> , Yasunori Yamamoto <sup>2</sup> ,  
Takuya Isono <sup>2,\*</sup>  and Toshifumi Satoh <sup>2,\*</sup> 

<sup>1</sup> Graduate School of Chemical Sciences and Engineering, Hokkaido University, Sapporo 060-8628, Japan; saburou\_k@eis.hokudai.ac.jp (S.K.); m\_ashiya630@eis.hokudai.ac.jp (M.A.)

<sup>2</sup> Faculty of Engineering, Hokkaido University, Sapporo 060-8628, Japan; yamamoto.t@eng.hokudai.ac.jp (T.Y.); ktajima@eng.hokudai.ac.jp (K.T.); yasuyama@eng.hokudai.ac.jp (Y.Y.)

\* Correspondence: isono.t@eng.hokudai.ac.jp (T.I.); satoh@eng.hokudai.ac.jp (T.S.)

**Abstract:** Herein, we report the Suzuki–Miyaura catalyst-transfer polycondensation (SCTP) of triolborate-type carbazole monomers, i.e., potassium 3-(6-bromo-9-(2-octyldodecyl)-9H-carbazole-2-yl)triolborate (**M1**) and potassium 2-(7-bromo-9-(2-octyldodecyl)-9H-carbazole-2-yl) triolborate (**M2**), as an efficient and versatile approach for precisely synthesizing poly[9-(2-octyldodecyl)-3,6-carbazole] (3,6-PCz) and poly[9-(2-octyldodecyl)-2,7-carbazole] (2,7-PCz), respectively. The SCTP of triolborate-type carbazole monomers was performed in a mixture of THF/H<sub>2</sub>O using an initiating system consisted of 4-iodobenzyl alcohol, Pd<sub>2</sub>(dba)<sub>3</sub>•CHCl<sub>3</sub>, and *t*-Bu<sub>3</sub>P. In the SCTP of **M1**, cyclic by-product formation was confirmed, as reported for the corresponding pinacolboronate-type monomer. By optimizing the reaction temperature and reaction time, we successfully synthesized linear end-functionalized 3,6-PCz for the first time. The SCTP of **M2** proceeded with almost no side reaction, yielding 2,7-PCz with a functional initiator residue at the  $\alpha$ -chain end. Kinetic and block copolymerization experiments demonstrated that the SCTP of **M2** proceeded in a chain-growth and controlled/living polymerization manner. This is a novel study on the synthesis of 2,7-PCz via SCTP. By taking advantage of the well-controlled nature of this polymerization system, we demonstrated the synthesis of high-molecular-weight 2,7-PCzs ( $M_n = 5\text{--}38 \text{ kg mol}^{-1}$ ) with a relatively narrow  $D_M$  (1.35–1.48). Furthermore, we successfully synthesized fluorene/carbazole copolymers as well as 2,7-PCz-containing diblock copolymers, demonstrating the versatility of the present polymerization system as a novel synthetic strategy for well-defined polycarbazole-based materials.

**Keywords:**  $\pi$ -conjugated polymer; polycarbazole; catalyst-transfer polycondensation



**Citation:** Kobayashi, S.; Ashiya, M.; Yamamoto, T.; Tajima, K.; Yamamoto, Y.; Isono, T.; Satoh, T. Suzuki–Miyaura Catalyst-Transfer Polycondensation of Triolborate-Type Carbazole Monomers. *Polymers* **2021**, *13*, 4168. <https://doi.org/10.3390/polym13234168>

Academic Editor: Bożena Jarzabek

Received: 3 November 2021

Accepted: 25 November 2021

Published: 28 November 2021

**Publisher's Note:** MDPI stays neutral with regard to jurisdictional claims in published maps and institutional affiliations.



**Copyright:** © 2021 by the authors. Licensee MDPI, Basel, Switzerland. This article is an open access article distributed under the terms and conditions of the Creative Commons Attribution (CC BY) license (<https://creativecommons.org/licenses/by/4.0/>).

## 1. Introduction

$\pi$ -Conjugated polymers have attracted immense attention owing to their potential as electroactive and photoactive materials for fabricating various organic electronic devices [1,2] such as organic light-emitting diodes (OLEDs) [3,4], organic field-effect transistors (OFETs) [5,6], organic photovoltaics (OPVs) [7,8], and organic memory devices [9–11]. Most  $\pi$ -conjugated polymers investigated thus far consisted of thiophene [12–16], phenylene [17–19], and fluorene [20–23] units, which have been accessed through the step-growth polycondensations using cross-coupling reactions, such as Suzuki–Miyaura and Kumada–Corriu coupling. However, precise control of the molecular weight, dispersity ( $D_M$ ), and end group of the  $\pi$ -conjugated polymers has been challenging due to the step growth nature of the polymerization. On the other hand, Yokozawa and McCullough established chain-growth-type catalyst-transfer polycondensation based on Kumada coupling and Suzuki–Miyaura coupling in 2001 [24], 2005 [25], and 2006 [26], respectively. This novel polymerization mechanism opened the access to a range of  $\pi$ -conjugated polymers with a predictable molecular weight, low  $D_M$ , and defined end groups.

Among the approaches to give  $\pi$ -conjugated polymers, catalyst transfer polymerization for polycarbazoles has not been extensively studied. Polycarbazoles can be distinguished based on the bonding positions of repeating units [27]. Poly(*N*-alkyl-3,6-carbazole)s (3,6-PCz), with an *m*-phenylene-like configuration, have been applied to OLEDs, flash memory devices, and devices utilizing thermally activated delayed fluorescence [28–32]. In contrast, poly(*N*-alkyl-2,7-carbazole)s (2,7-PCz), possessing a *p*-phenylene-like configuration, have been used in OLEDs and OPV devices [33–38]. Despite their promising potential in many applications, the synthesis of polycarbazoles relies on the polycondensation of symmetric bifunctional monomers (i.e., A–A + B–B type reaction, where the A and B mean complementary reactive groups) [39,40]. However, there are only a few examples of chain-growth-type catalyst transfer polycondensation for synthesizing poly(*N*-alkyl-carbazole)s [41]. Tan et al. first reported the synthesis of poly(*N*-heptadecan-2,7-carbazole) and poly(*N*-octyl-3,6-carbazole) via Kumada catalyst-transfer polycondensation (KCTP) [42]. However, the poor functional group tolerance of the Grignard-type monomers used in KCTP limited the application of functional initiators to introduce reactive functional groups on the chain end. In contrast, due to the good functional group tolerance of organoboron species, Suzuki–Miyaura catalyst-transfer polycondensation (SCTP) is highly attractive for the precise synthesis of poly(*N*-alkyl-carbazole)s with functional end groups. Jager et al. reported the synthesis of an end-functionalized poly(*N*-octyl-3,6-carbazole) via the SCTP of a pinacolboronate-type monomer [43]. However, a chain transfer reaction occurred during polymerization, leading to the formation of macrocyclic by-products and polymers with undesired end groups. To the best of our knowledge, the SCTP synthesis of 2,7-PCz has never been reported. This offers room to further investigate control of the SCTP to precisely synthesize 3,6- and 2,7-PCzs with desired molecular weights, narrow  $D_M$ , and end groups. Accordingly, we focused on triolborate-type monomers, which possess higher nucleophilicity than conventional pinacolboronate-type monomers. Triolborate salts are known to show higher reactivity than other organoboron reagents [44,45], enabling reactions with heteroaromatic and alkyl compounds [46–48], which are typically inactive in Suzuki–Miyaura coupling. In addition, triolborate salts show good solubility in common organic solvents and are air-/water-stable, and hence, they can be applied for Suzuki–Miyaura coupling without the addition of water and a base. By utilizing these characteristics, we recently reported the SCTP of a triolborate salt-type fluorene monomer, which successfully compensated for the shortcomings encountered in the SCTP of conventional pinacolboronate fluorene monomers [49].

In this study, we investigated the SCTP of triolborate salt carbazole monomers, i.e., potassium 3-(6-bromo-9-(2-octyldodecyl)-9*H*-carbazole-2-yl) triolborate (**M1**) and potassium 2-(7-bromo-9-(2-octyldodecyl)-9*H*-carbazole-2-yl) triolborate (**M2**), with the aim of establishing a synthetic approach for well-defined 3,6-PCzs and 2,7-PCzs. We successfully achieved the selective synthesis of end-functionalized 3,6-PCz by the SCTP of **M1** at low temperatures to suppress the chain transfer reaction. The SCTP of **M2** proceeded in chain growth and a controlled/living polymerization mechanism to produce 2,7-PCzs with controlled molecular weights (5080–37,900 g mol<sup>−1</sup>) and a relatively narrow  $D_M$  (1.35–1.48). Using the established SCTP conditions, we successfully synthesized random copolymers of *N*-alkyl-3,6- and 2,7-carbazoles, random copolymers of *N*-alkyl-carbazole and 9,9-dialkylfluorene, and 2,7-PCz-containing block copolymers.

## 2. Materials and Methods

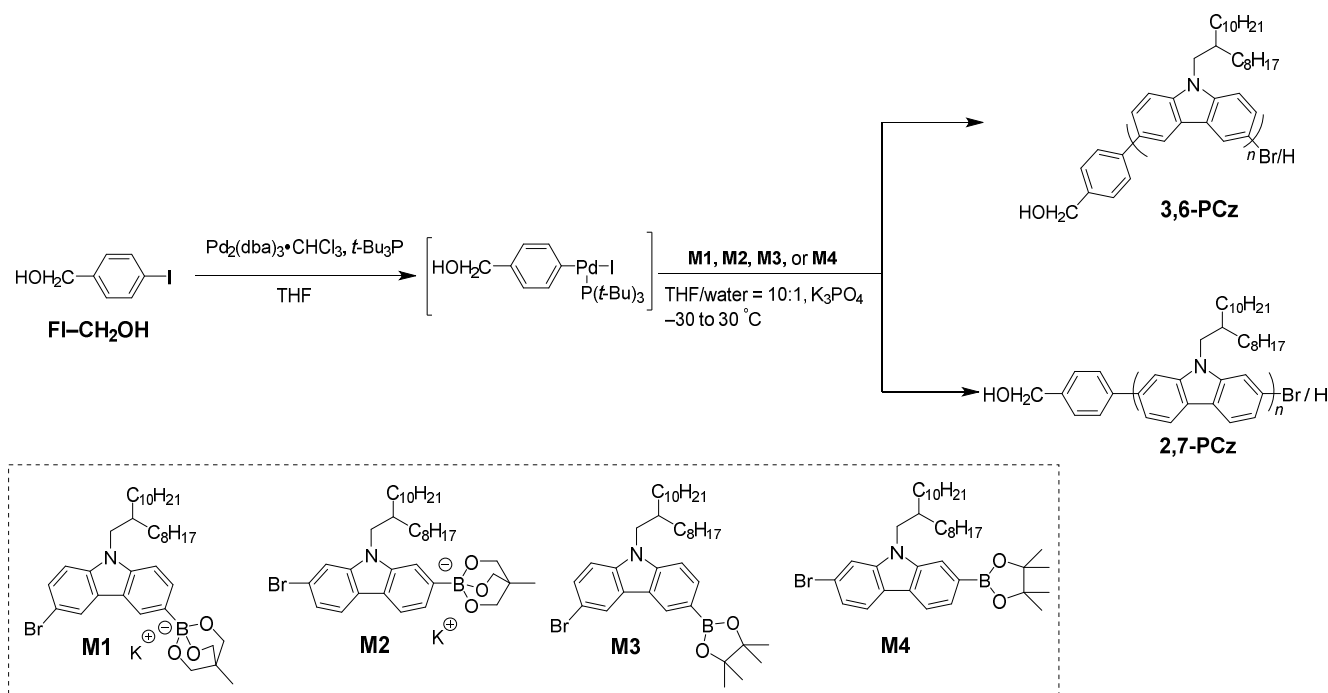
The Materials and Methods are described in the Supplementary Materials.

## 3. Results and Discussion

### 3.1. SCTP of M1 to Produce 3,6-PCz

We first investigated the synthesis of end-functionalized poly[9-(2-octyldodecyl)-3,6-carbazole] (3,6-PCz) with a narrow dispersity ( $D_M$ ). Recently, Jager et al. demonstrated the synthesis of 3,6-PCzs by the SCTP of a pinacol boronate-type monomer, using bro-

mobenzene derivative as the initiator [43]. However, a significant amount of macrocyclic byproduct was generated owing to the chain transfer reaction, in addition to the desired linear polymer obtained from the bromobenzene derivative. We hypothesized that the chain transfer reaction can be suppressed by using triolborate salt monomers because of its high reactivity even at low temperatures, resulting in suppressed cyclization side reactions (Scheme 1).



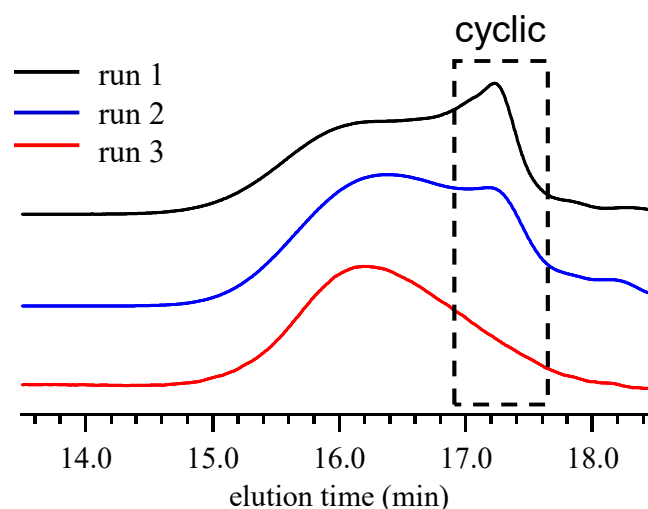
**Scheme 1.** Synthesis scheme for the end-functionalized PCzs based on the SCTP of triolborate-type carbazole monomers.

We first attempted the polymerization of potassium 3-(6-bromo-9-(2-octyldodecyl)-9H-carbazole-2-yl)triolborate (**M1**) using an initiating system that consisted of 4-iodobenzyl alcohol (**FI-CH<sub>2</sub>OH**), Pd<sub>2</sub>(dba)<sub>3</sub>•CHCl<sub>3</sub>, and *t*-Bu<sub>3</sub>P, with an [**M1**]<sub>0</sub>/[**FI-CH<sub>2</sub>OH**]<sub>0</sub>/[Pd<sub>2</sub>(dba)<sub>3</sub>•CHCl<sub>3</sub>]/[*t*-Bu<sub>3</sub>P]/[K<sub>3</sub>PO<sub>4</sub>] ratio of 15/1/0.3/2.2/1.5 at 30 °C in a mixture of THF/water (10:1; *v/v*, [**M1**]<sub>0</sub> = 10 mmol L<sup>-1</sup>), based on the previously established conditions for polyfluorene synthesis [49]. Although SCTP proceeded to afford 3,6-PCz (*M<sub>n,SEC</sub>* = 5500 g mol<sup>-1</sup>), the size-exclusion chromatography (SEC) analysis revealed a bimodal distribution with a dispersity (*D<sub>M</sub>*) of 1.32 (run 1, Table 1, Figure 1). The structure of the 3,6-PCz was investigated using matrix-assisted laser desorption/ionization time-of-flight mass spectroscopy (MALDI-TOF MS). As shown in Figure 2, the MALDI-TOF mass spectrum exhibited six series of peaks with a regular interval of 445.47 Da, corresponding to 9-(2-octyldodecyl) carbazole repeating units. One of the observed series of peaks was assigned to HOCH<sub>2</sub>-3,6-PCz with a phenylmethanol residue at the α-chain end and a bromine atom at the ω-chain end (BrOH/Br); for example, the peak of 1969.43 at *m/z* matched well with the theoretical mass for the 4-mer of HOCH<sub>2</sub>-3,6-PCz ([**M** + H]<sup>+</sup> = 1971.46 Da). However, peaks corresponding to 3,6-PCz with hydrogen and bromine ends (Br/H; e.g., *m/z* of 1864.42 Da), bromine at both ends (Br/Br; e.g., *m/z* of 1942.31 Da), and cyclic 3,6-PCz (e.g., *m/z* = 1783.50 Da) were observed, revealing the uncontrolled polymerization nature.

**Table 1.** SCTP of triolborate-type carbazole monomers under various conditions <sup>a</sup>.

Run	Monomer	[monomer] <sub>0</sub> /[FI–CH <sub>2</sub> OH] <sub>0</sub>	Temp (°C)	<i>M</i> <sub>n,SEC</sub> <sup>b</sup> (g mol <sup>−1</sup> )	<i>D</i> <sub>M</sub> <sup>b</sup>	Conv. (%)	Yield <sup>c</sup> (%)
1	M1	15/1	30	5500	1.32	83.2	80.6
2 <sup>d</sup>	M1	15/1	30	5900	1.30	74.2	65.2
3	M1	15/1	−10	6300	1.19	65.3	60.1
4	M1	15/1	−30	—	—	—	—
5	M3	15/1	−10	—	—	—	—
6	M2	15/1	30	3700	1.23	99.2	74.8
7	M2	15/1	−30	—	—	—	—
8	M2	15/1	−10	—	—	—	—
9	M4	15/1	30	—	—	—	—
10	M2	30/1	30	8600	1.35	98.6	74.2
11	M2	60/1	30	16,400	1.45	97.6	75.6
12	M2	90/1	30	32,000	1.48	96.4	73.2

<sup>a</sup> Polymerization condition: atmosphere, Ar; solvent, THF/water (10:1, v/v); [monomer]<sub>0</sub> = 10 mmol L<sup>−1</sup>; [FI–CH<sub>2</sub>OH]<sub>0</sub>/[Pd<sub>2</sub>(dba)<sub>3</sub>•CHCl<sub>3</sub>]/[*t*-Bu<sub>3</sub>P]/[K<sub>3</sub>PO<sub>4</sub>] = 1/0.3/2.2/1.5. <sup>b</sup> Determined by SEC using PSt standards. <sup>c</sup> Isolated yields. <sup>d</sup> *t*-Bu<sub>3</sub>P (4.4 equiv.).

**Figure 1.** SEC traces of 3,6-PCzs obtained from runs 1, 2, and 3 in Table 1).

According to a report by Jager et al. [43], the sharp SEC elution peaks observed in the lower-molecular-weight region and the relatively broad elution peak at high molecular weight in Figure S1 most likely arise from the cyclic by-product and linear polymer, respectively. The MALDI-TOF mass spectrum of the high-molecular-weight side, which was isolated by preparative SEC, predominantly showed peaks corresponding to 3,6-PCz, with a phenylmethanol residue at the end (Figure S1). Nevertheless, these results suggest that the chain transfer reaction occurred significantly, even with the triolborate-type monomer under this polymerization condition.

To inhibit the chain transfer reaction, we optimized the polymerization conditions for **M1**. Hong et al. reported the synthesis of polyfluorene with a narrow *D*<sub>M</sub> by SCTP with the addition of extra *t*-Bu<sub>3</sub>P [50]. Therefore, we conducted the polymerization of **M1** by adding 4.4 equiv. of *t*-Bu<sub>3</sub>P with respect to FI–CH<sub>2</sub>OH, without changing any other factors (run 2, Table 1). As a result, the SEC elution peak corresponding to the cyclic by-product was reduced compared to that in run 1, implying that the chain transfer reaction was suppressed to some extent (Figure 1). We also examined the polymerization by changing the phosphine ligand (e.g., dppp, XPhos, and RuPhos), but no positive results were obtained. Next, polymerization was carried out by lowering the reaction temperature (−30 °C and −10 °C) to further reduce the unwanted chain transfer reaction. For polymerization at −30 °C (run 4), **M1** precipitated during SCTP. In contrast, the polymer given at −10 °C (run 3) exhibited a nearly monomodal SEC elution peak with a

narrow dispersity of 1.19 (Figure 1). Consequently, lowering the reaction temperature was found to be an effective method to suppress the chain transfer reaction as well as cyclic by-product formation. For comparison, we examined the polymerization of a conventional pinacolboronate-type carbazole monomer, 3-(6-bromo-9-(2-octyldodecyl)-9H-carbazole-2-yl)4,4,5,5-tetramethyl-1,2,3-dioxaborolane (**M3**), under the same conditions as for **M1**. However, no polymerization was observed at  $-10\text{ }^{\circ}\text{C}$  (run 5, Table 1, Figure S3). This result demonstrates that the SCTP of the triolborate salt monomer at low temperatures is essential for the controlled synthesis of 3,6-PCz.

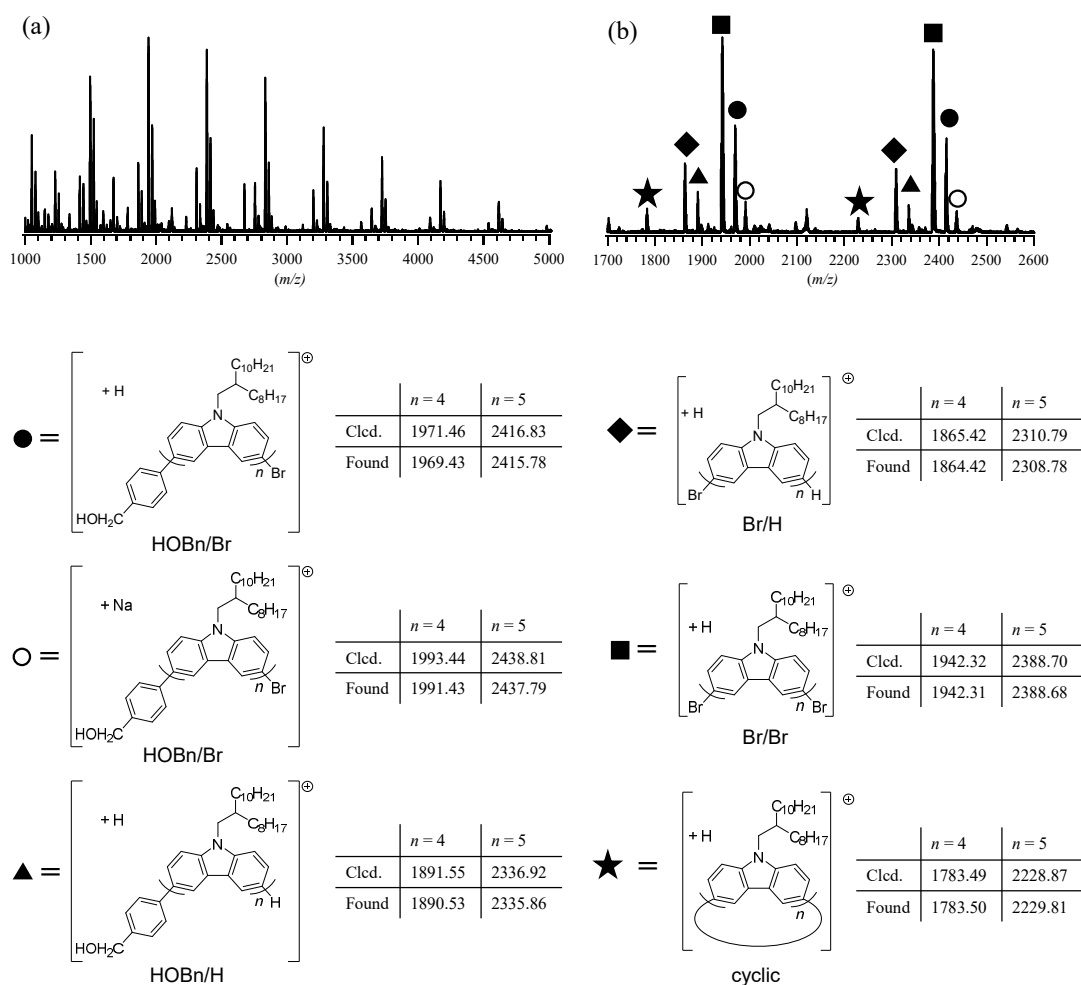


**Figure 2.** MALDI-TOF mass spectral analysis of  $\text{HOCH}_2\text{-3,6-PCz}$  obtained from run 1 (Table 1). (a) MALDI-TOF mass spectrum. (b) Expanded spectrum ranging from 1700 to 2600 Da.

The structure of 3,6-PCz obtained at  $-10\text{ }^{\circ}\text{C}$  (run 3) was characterized in detail by NMR and mass spectral analyses. In the  $^1\text{H}$  NMR spectrum (Figure 3a), the major signals were successfully assigned to the 3,6-PCz backbone (8.65–7.31 ppm: proton A) and 2-octyldodecyl side chain (2.11 ppm: proton B, 4.12 ppm: proton C, 1.82–0.75 ppm: proton D and E), which is consistent with the reported  $^1\text{H}$  NMR data for poly[9-(2-octyl)-3,6-carbazole] synthesized via SCTP [43]. More importantly, a minor signal due to the benzyl proton (proton F) in the  $\alpha$ -chain end group was observed at 4.75 ppm, indicating the initiation from  $\text{FI-CH}_2\text{OH}$ . Thus, the obtained product was identified as the expected poly[9-(2-octyldodecyl)-3,6-carbazole] possessing a phenylmethanol residue at the  $\alpha$ -chain end ( $\text{HOCH}_2\text{-3,6-PCz}$ ). The number-average molecular weight ( $M_{n,\text{NMR}}$ ) of the  $\text{HOCH}_2\text{-3,6-PCz}$  (run 3), determined based on end group analysis of the  $^1\text{H}$  NMR spectrum, was  $6700\text{ g mol}^{-1}$ . In order to confirm the end-group fidelity, we performed MALDI-TOF MS analysis on this sample. The MALDI-TOF mass spectrum showed two series of peaks with

a regular interval of 445.47 Da, corresponding to 9-(2-octyldodecyl) carbazole repeating units (Figure 3b). The peaks indicated by filled circles (●) were assignable to HOCH<sub>2</sub>–3,6-PCz possessing a phenylmethanol residue at the  $\alpha$ -chain end and a bromine atom at the  $\omega$ -chain end (BnOH/Br); for example, the peak at  $m/z$  of 1970.40 showed good agreement with the theoretical mass for the 4-mer ( $[M + H]^+ = 1970.46$  Da). The peaks indicated by filled triangles (▲) were assignable to HOCH<sub>2</sub>–3,6-PCz possessing a phenylmethanol residue at the  $\alpha$ -chain end and a hydrogen atom  $\omega$ -chain end (BnOH/H). Overall, the SCTP of **M1** at low temperature enables better control, yielding narrowly dispersed 3,6-PCzs with sufficient end-group fidelity.

To understand the polymerization properties of **M1**, we evaluated the time-dependent change of the reaction product via the SEC and MALDI-TOF MS analysis of the crude aliquot quenched by the addition of HCl (1 mol L<sup>-1</sup>). SEC did not confirm an increase in molecular weight over time, as expected for chain growth polycondensation (Figure 4). This suggests that the polymerization of **M1** does not proceed in a perfect living fashion, even with the best polymerization conditions. It is reasonable to deduce that various side reactions occur in this polymerization system. MALDI-TOF MS analysis revealed a complex polymerization behavior. From the beginning of polymerization to 5 h, 3,6-PCz with HOBn/Br ( $m/z$  of 1969.3 Da) and HOBn/H ( $m/z$  of 1969.3 Da) chain end structures were the major products, suggesting that polymerization was initiated from the palladium 4-iodobenzyl alcohol[tris(1,1-dimethylethyl)phosphine] (iodobenzyl alcohol-Pd) complex, as expected. However, when polymerization continued thereafter, the populations of 3,6-PCz with Br/Br ( $m/z$  of 1943.1 Da) and Br/H ( $m/z$  of 1863.3 Da) chain end structures increased over time (Figure 5 and Figure S2). This complex polymerization behavior can be explained as shown in Scheme 2. The first step of polymerization involves the transmetalation between the initiator and monomer to yield the Pd complex (i) when the Pd(0) species, which are generated by reductive elimination, are intramolecularly shifted to the carbon–bromine bond at the end of the same molecule. Polymerization proceeds via chain growth from (ii), resulting in the formation of 3,6-PCz with a phenylmethanol residue at the initiation end (HOBn/Br or HOBn/H) (Scheme 2a). However, when the Pd(0) species does not shift to the bromine end in the same molecule but intramolecularly shifts to the new monomer, a new initiating species (iii) is generated [51–54]. The initiating species (iii) generates 3,6-PCz with a triolborate residue at the  $\alpha$ -chain end and bromine atom at the  $\omega$ -chain end, which results in the formation of the cyclic by-product though the intramolecular reaction. Meanwhile, when the Pd catalyst is oxidized by a trace amount of oxygen [55,56], the homocoupling of two monomer molecules (iv) produces another initiating species, which results in the formation of 3,6-PCz at the brominated  $\alpha$ -chain end (Br/Br and Br/H) (Scheme 2b).

Overall, even the polymerization of the triolborate-type monomer **M1** did not proceed in a perfect fashion. Nevertheless, we successfully obtained 3,6-PCz with the desired initiator residue virtually without contamination of the cyclic by-product, by optimizing the polymerization temperature and time.

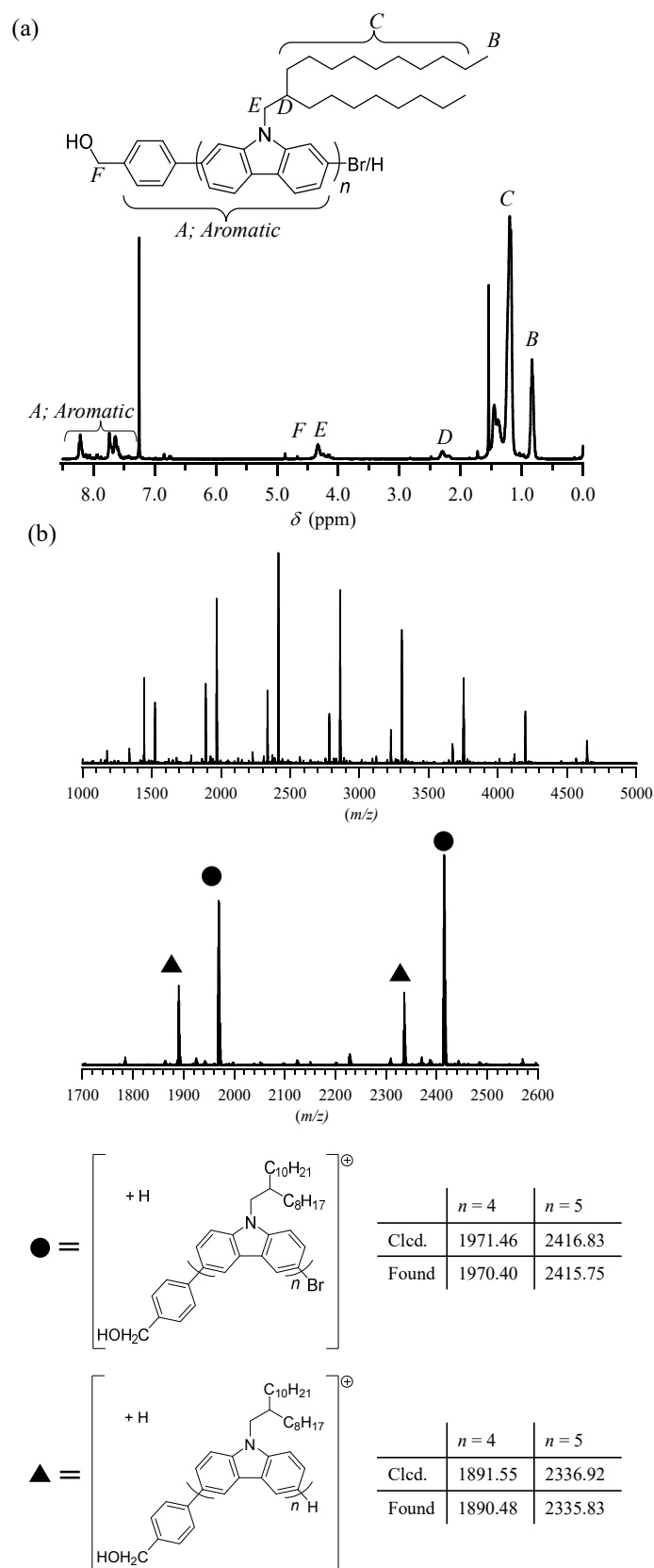


**Figure 3.**  $^1\text{H}$  NMR and MALDI-TOF mass spectral analysis of  $\text{HOCH}_2\text{-3,6-PCz}$  obtained from run 3 (Table 1). (a)  $^1\text{H}$  NMR in  $\text{CDCl}_3$  (400 MHz). (b) MALDI-TOF mass spectrum with peak assignments.

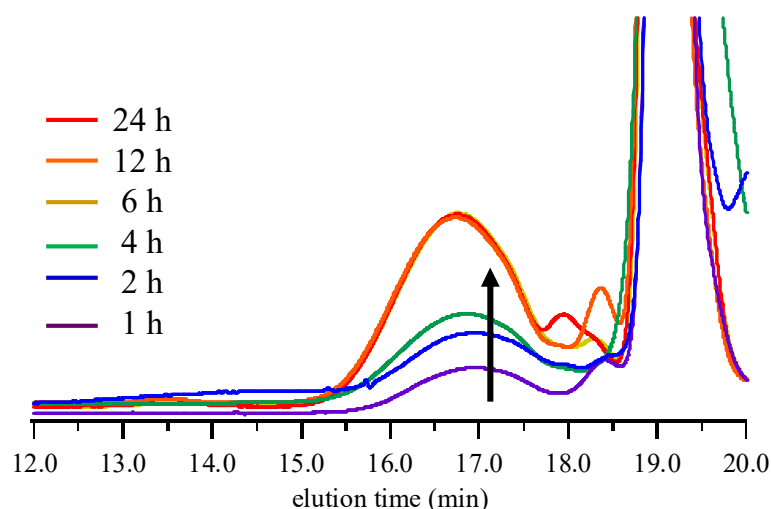


**Figure 4.** SEC traces of crude aliquot collected from the polymerization mixture of **M1** at selected times.

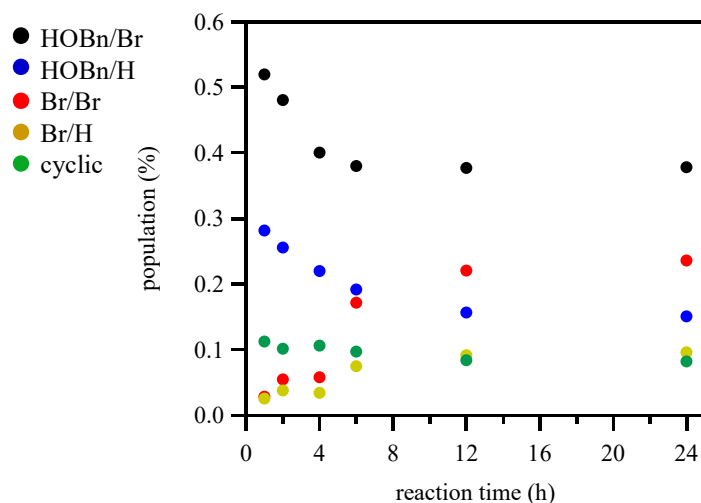
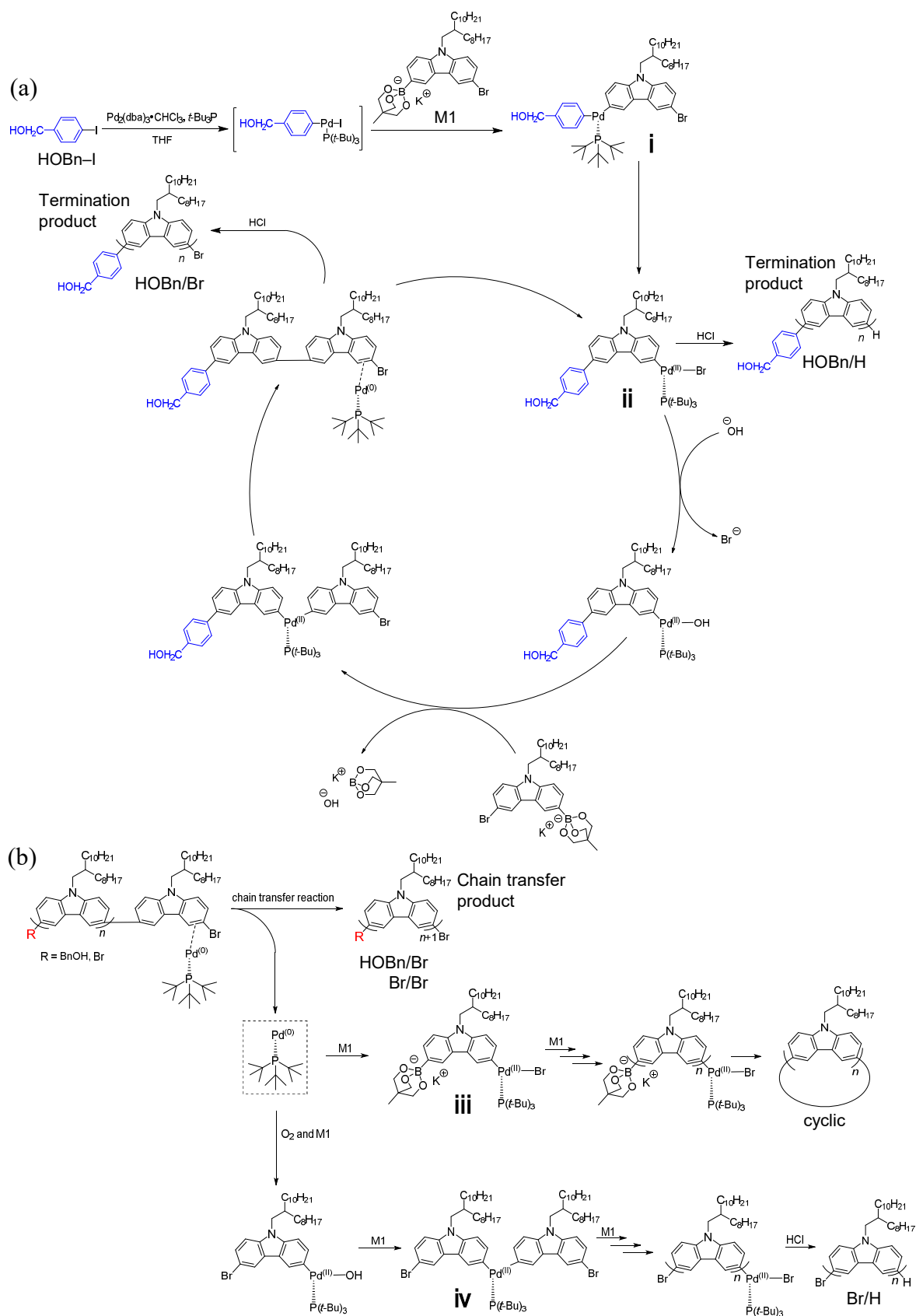


**Figure 5.** Evolution of 3,6-PCz species with different chain ends over time, as determined by MALDI-TOF MS analysis.

### 3.2. SCTP of **M2** to Produce 2,7-PCz

Next, we investigated the polymerization of potassium 2-(7-bromo-9-(2-octyldodecyl)-9*H*-carbazole-2-yl)triolborate (**M2**). The initial attempt was carried out using an initiating system that consisted of **FI-CH<sub>2</sub>OH**, Pd<sub>2</sub>(dba)<sub>3</sub>•CHCl<sub>3</sub>, and *t*-Bu<sub>3</sub>P with an [M<sub>2</sub>]<sub>0</sub>/[FI-CH<sub>2</sub>OH]<sub>0</sub>/[Pd<sub>2</sub>(dba)<sub>3</sub>•CHCl<sub>3</sub>]/[*t*-Bu<sub>3</sub>P]/[K<sub>3</sub>PO<sub>4</sub>] ratio of 15/1/0.3/2.2/1.5 at 30 °C in a mixture of THF/water (10:1; *v/v*, [M<sub>2</sub>]<sub>0</sub> = 10 mmol L<sup>-1</sup>) (Scheme 1; run 6 in Table 1), according to the best polymerization conditions for potassium 2-(7-bromo-9,9-dihexyl-9*H*-fluorene-2-yl)triolborate [49]. The SCTP of **M2** successfully proceeded to afford a polymer with  $M_{n,SEC} = 3700 \text{ g mol}^{-1}$  and  $D_M = 1.23$ . To study the effect of the polymerization temperature, we carried out SCTP at -30 °C and -10 °C while fixing the other reaction parameters. At -30 °C (run 7), the monomer and product precipitated during the SCTP. Meanwhile, at -10 °C (run 8), a low monomer conversion was observed even after polymerization for 24 h. Consequently, it became apparent that **M2** should be performed at 30 °C. For comparison, we examined the SCTP of a conventional pinacolboronate-type monomer, i.e., 2-(7-bromo-9-(2-octyldodecyl)-9*H*-carbazole-2-yl)4,4,5,5-tetramethyl-1,2,3-dioxaborolane (**M4**) under the comparable condition (run 9). As a result, no polymerization was observed even after 24 h. This result demonstrates the advantage of using a triolborate salt monomer for the synthesis of 2,7-PCz.





Then, the structure of the obtained 2,7-PCz was characterized in detail by NMR and MALDI-TOF mass spectral analyses. Figure 6a shows the  $^1\text{H}$  NMR spectrum of the product obtained from run 6. The major observed signals were reasonably assignable to the 2,7-PCz backbone (8.68–7.33 ppm: proton A) and 2-octyldodecyl side chain (2.12 ppm: proton B, 4.14 ppm: proton C, 1.82–0.73 ppm: proton D and E), which is consistent with the reported  $^1\text{H}$  NMR data for poly[*N*-heptadecan-2,7-carbazole] synthesized via KCTP [42]. More importantly, a minor signal at 4.75 ppm was assigned to the benzyl proton at the  $\alpha$ -chain end (proton E), which confirmed the successful installation of the functional end group. Therefore, the obtained product was ascribed to the expected poly[9-(2-octyldodecyl)-2,7-carbazole] possessing a phenylmethanol residue at the  $\alpha$ -chain end ( $\text{HOCH}_2$ -2,7-PCz). The  $M_{n,\text{NMR}}$  of  $\text{HOCH}_2$ -2,7-PCz (run 6) was calculated to be  $5080 \text{ g mol}^{-1}$  by end-group analysis of the  $^1\text{H}$  NMR spectrum. In order to further confirm the end-group fidelity, we performed MALDI-TOF MS analysis on the product from run 6. The MALDI-TOF mass spectrum mainly exhibited two series of peaks showing a regular interval of 445.4 Da corresponding to 9-(2-octyldodecyl) carbazole repeating units (Figure 6b). The peaks denoted by filled triangles ( $\blacktriangle$ ) were assignable to  $\text{HOCH}_2$ -2,7-PCz possessing a phenylmethanol residue at the  $\alpha$ -chain end and a bromine atom at the  $\omega$ -chain end. For example, the peak at  $m/z = 2415.75$  matched with the theoretical mass for the 5-mer (BnOH/Br;  $[M + H]^+ = 2416.83 \text{ Da}$ ). The peaks denoted by filled circles ( $\bullet$ ) were assigned to  $\text{HOCH}_2$ -2,7-PCz possessing a phenylmethanol residue at the  $\alpha$ -chain end and a hydrogen atom at the  $\omega$ -chain end (BnOH/H;  $[M + H]^+ = 2336.92 \text{ Da}$ ). Overall, in contrast to the case of **M1**, the SCTP of **M2** proceeded in a controlled/living fashion to give narrowly dispersed 2,7-PCzs with good end-group fidelity.

In order to demonstrate the chain growth and controlled/living polymerization behaviors in the SCTP of **M2**, we carried out kinetic and block copolymerization experiments (Scheme 3). For the kinetic study, the polymerization of **M2** using **FI-CH<sub>2</sub>OH** was performed in a mixture of THF/water (10:1, *v/v*,  $[\text{M2}]_0 = 10 \text{ mmol L}^{-1}$ ) at  $30^\circ\text{C}$  with an  $[\text{M2}]_0/[\text{FI-CH}_2\text{OH}]_0/[\text{Pd}_2(\text{dba})_3\bullet\text{CHCl}_3]/[t\text{-Bu}_3\text{P}]/[\text{K}_3\text{PO}_4]$  ratio of 30/1/0.3/2.2/1.5. As shown in Figure 7a, polymerization proceeds smoothly, and >98% of the monomer is consumed within 12 h. Figure 7b reveals that the  $M_{n,\text{SEC}}$  of the obtained 2,7-PCz linearly increases with the increase in the monomer conversion, while the  $D_M$  values remain narrow ( $D_M < 1.4$ ). This is strong evidence for the chain-growth mechanism of the SCTP. The kinetic plot indicates a distinct first-order kinetic behavior for this polymerization system. According to slope of the kinetic plot, the rate constant was estimated to be  $5.8 \text{ s}^{-1} \text{ mmol L}^{-1}$  (Figure 7c). A block copolymerization experiment was further carried out to prove the controlled/living nature of the propagating end of 2,7-PCz. **M2** was first polymerized for 12 h with an  $[\text{M2}]_0/[\text{FI-CH}_2\text{OH}]_0/[\text{Pd}_2(\text{dba})_3\bullet\text{CHCl}_3]/[t\text{-Bu}_3\text{P}]/[\text{K}_3\text{PO}_4]$  ratio of 15/1/0.3/2.2/1.5, to yield an intermediate 2,7-PCz with an  $M_{n,\text{SEC}}$  of  $3700 \text{ g mol}^{-1}$  and  $D_M$  of 1.23. After confirming full monomer conversion, 15 equiv. of potassium 2-(7-bromo-9,9-dihexyl-9H-fluorene-2-yl)triolborate (**M5**) was added for chain extension, which afforded 2,7-PCz-*b*-PF with  $M_{n,\text{NMR}}$  of  $9400 \text{ g mol}^{-1}$  and a  $D_M$  of 1.38. The SEC traces of the products before and after block copolymerization are shown in Figure 7d, in which the SEC elution peak showed clear shift toward the high-molecular-weight side upon the addition of the second monomer. This result verified a truly controlled/living propagating end, which led to chain extension by the second monomer addition. Overall, the aforementioned results successfully support the chain-growth and controlled/living polymerization nature of the SCTP of **M2**.

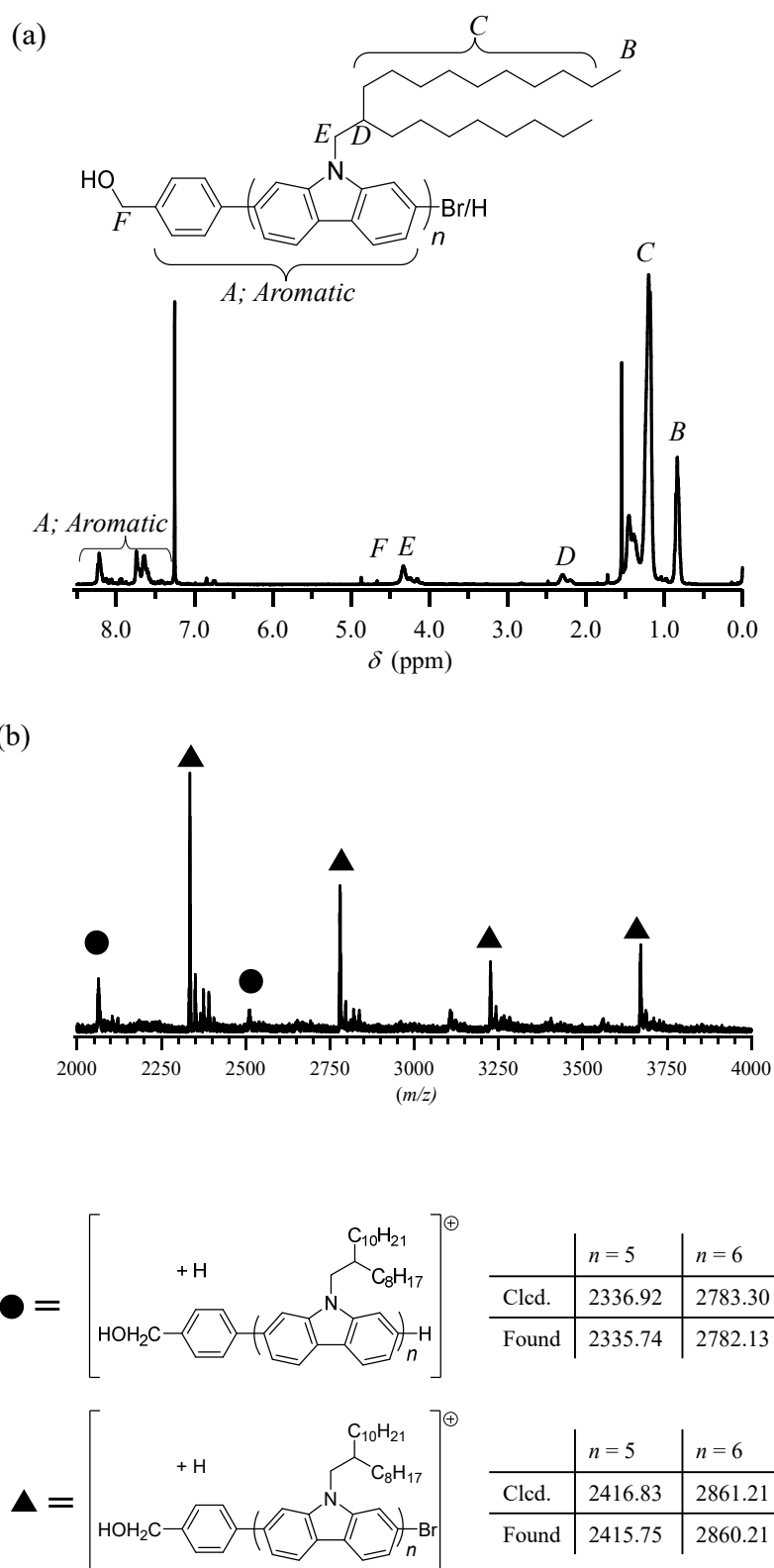
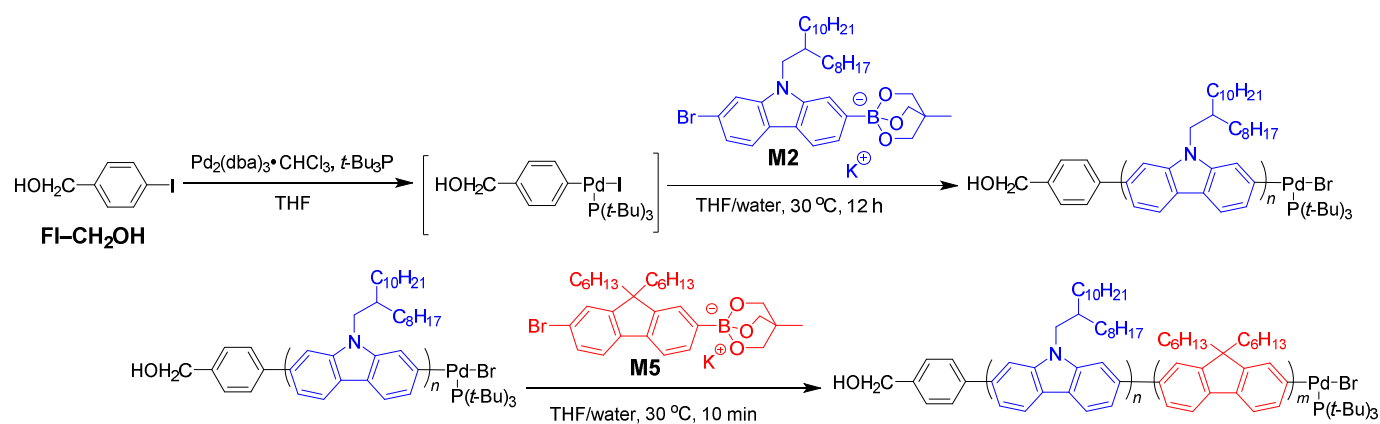


**Figure 6.**  $^1\text{H}$  NMR and MALDI-TOF mass spectral analysis on  $\text{HOCH}_2\text{-2,7-PCz}$  obtained from run 6 (Table 1) (a)  $^1\text{H}$  NMR in  $\text{CDCl}_3$  (400 MHz). (b) MALDI-TOF mass spectrum with peak assignments.



**Scheme 3.** Block copolymerization experiment to confirm controlled/living nature in the SCTP of **M2**.

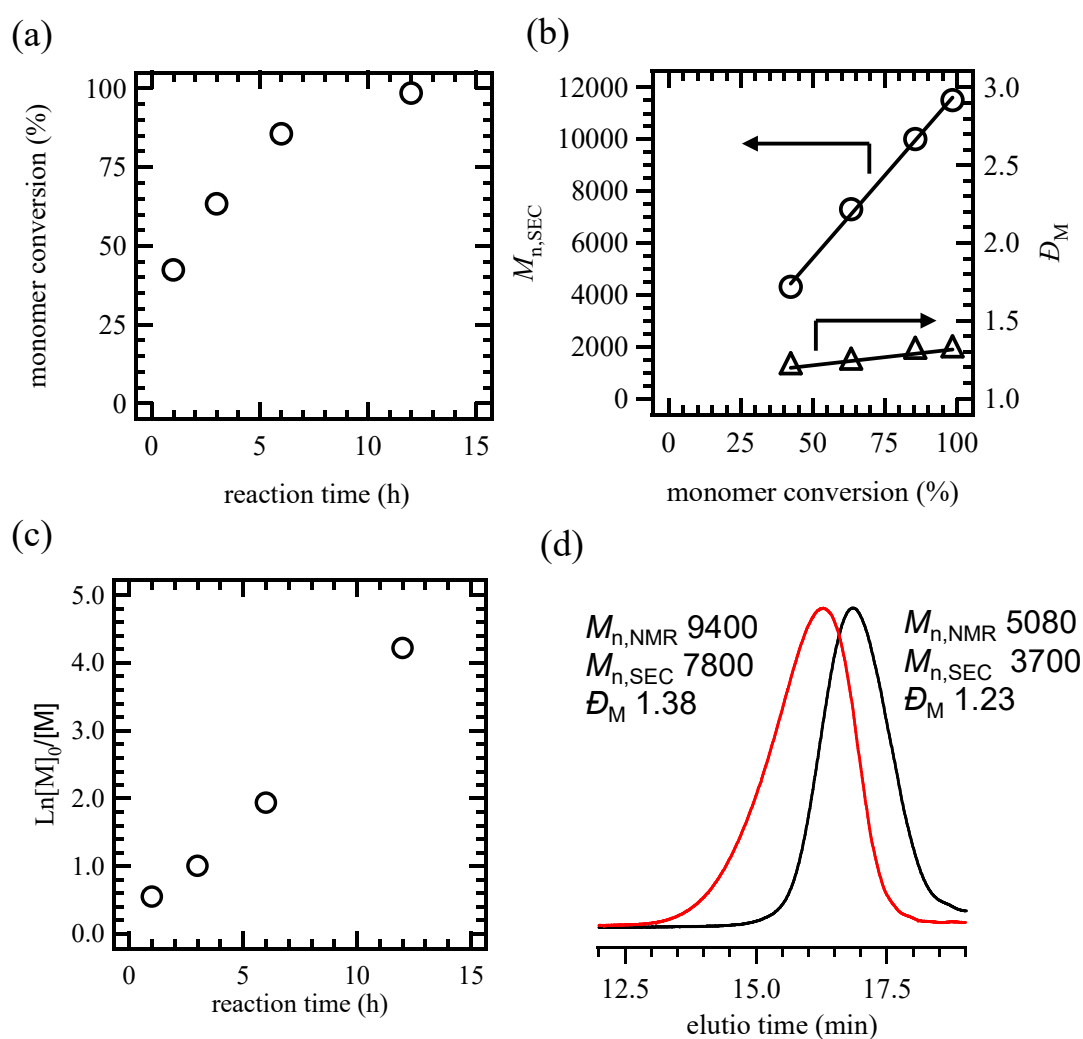


**Figure 7.** (a) Time-conversion plot in the SCTP of **M2** ( $[\text{M2}]_0/[\text{FI-CH}_2\text{OH}]_0/[\text{Pd}_2(\text{dba})_3 \cdot \text{CHCl}_3]/[t\text{-Bu}_3\text{P}]/[\text{K}_3\text{PO}_4] = 15:1:0.3:2.2:1.5$ ; solvent, THF/water (10:1,  $v/v$ ); temp., 30 °C). (b) Dependence of  $M_{n,SEC}$  and  $\bar{D}_M$  on the monomer conversion. (c) Kinetic plots for SCTP. (d) SEC traces of 2,7-PCz (black line) and 2,7-PCz-*b*-PF obtained after the second polymerization (red line).

With the optimized polymerization conditions, the SCTP of **M2** was performed with different  $[\text{M2}]_0/[\text{FI-CH}_2\text{OH}]_0$  ratio (30/1 for run 10, 60/1 for run 11, and 90/1 for run 12) to synthesize 2,7-PCzs with different molecular weights. Thus, 2,7-PCzs with  $M_{n,SEC}$

and  $D_M$  values of 8600–32,000 g mol<sup>-1</sup> and 1.35–1.48, respectively (runs 10–12, Table 1,  $M_{n,NMR}$ ; 5080–37,900 g mol<sup>-1</sup>) were successfully obtained (Figure 8). To the best of our knowledge, 2,7-PCz obtained from run 12 ( $M_{n,SEC}$  of 37,900 g mol<sup>-1</sup>) had the highest molecular weight among the poly[9-(2-octyldodecyl)-2,7-carbazoles] prepared by chain-growth polycondensation.

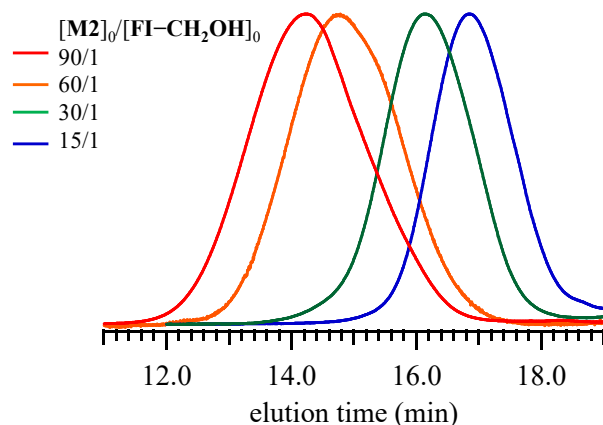


Figure 8. SEC traces of HOCH<sub>2</sub>-2,7-PCz obtained with different [M<sub>2</sub>]<sub>0</sub>/[FI-CH<sub>2</sub>OH]<sub>0</sub> ratios.

### 3.3. Random Copolymerization of Triolborate-Type Carbazole and Fluorene Monomers

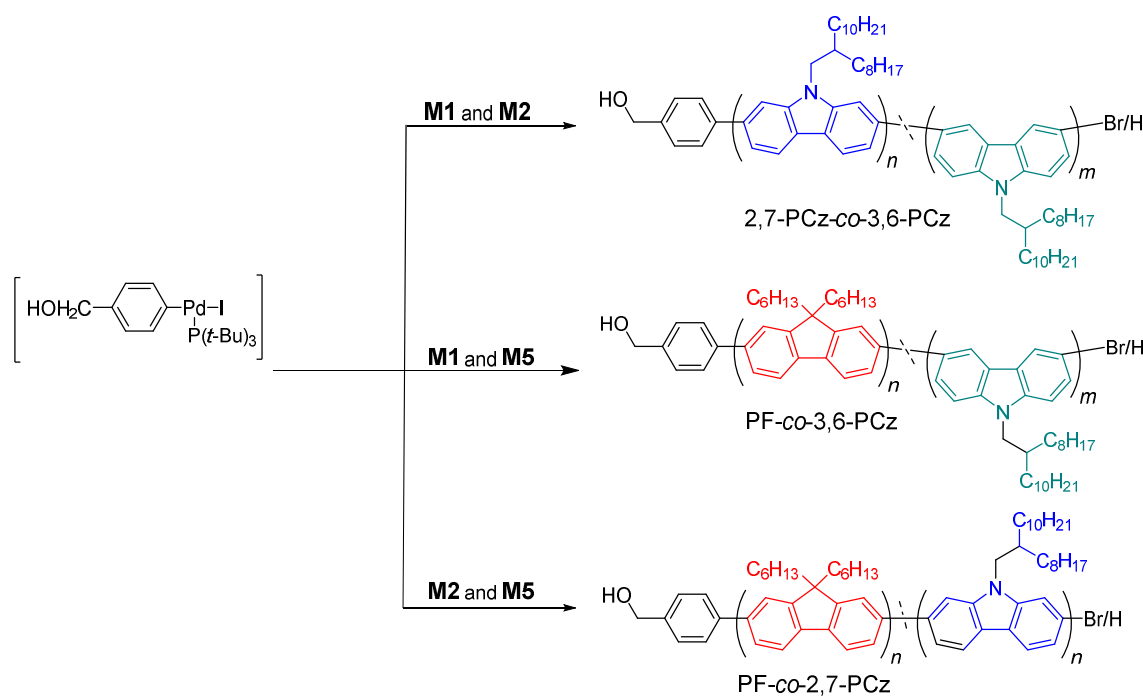
Recently, conjugated copolymers based on carbazole or fluorene groups with varying connectivity, such as at the 2,7 or 3,6 positions, were found to be useful for the extraction of single-walled carbon nanotubes [57]. Therefore, we are interested in testing our SCTP system for the synthesis of poly(carbazole-co-fluorene)s (Scheme 4). First, we examined the random copolymerization of M1 and M2 using the initiating system that consisted of FI-CH<sub>2</sub>OH, Pd<sub>2</sub>(dba)<sub>3</sub>•CHCl<sub>3</sub>, and *t*-Bu<sub>3</sub>P, at an [M1]/[M2]/[FI-CH<sub>2</sub>OH]<sub>0</sub>/[Pd<sub>2</sub>(dba)<sub>3</sub>•CHCl<sub>3</sub>]/[*t*-Bu<sub>3</sub>P]/[K<sub>3</sub>PO<sub>4</sub>] ratio of 15/15/1/0.3/2.2/1.5, at 30 °C in a mixture of THF/water (10:1; *v/v*, [monomers]<sub>0</sub> = 10 mmol L<sup>-1</sup>) (run 13, Table 2 run 13). SCTP proceeded to afford 2,7-PCz-co-3,6-PCz ( $M_{n,SEC}$  = 7800 g mol<sup>-1</sup>), which exhibited a unimodal SEC elution peak (Figure 9). The chemical structure of 2,7-PCz-co-3,6-PCz was identified by <sup>1</sup>H NMR analysis (Figure 10). The major signals were assigned to the polycarbazole backbone (8.6–7.3 ppm: proton A) and 2-octyldodecyl side chain (2.1 ppm: proton B, 4.1 ppm: proton C, 1.8–0.7 ppm: proton D and E). More importantly, a minor signal at 4.7 ppm due to the  $\alpha$ -chain end benzyl proton (proton F) was clearly observed, confirming the successful installation of the functional end group. Therefore, the product identified to be the expected copolymer possessed a phenylmethanol residue at the  $\alpha$ -chain end (2,7-PCz-co-3,6-PCz). The ratio of the 2,7-carbazole unit to the 3,6-carbazole unit in the obtained copolymer was 14:14, which was in good agreement with the monomer feed ratio. The  $M_{n,NMR}$  of 2,7-PCz-co-3,6-PCz (run 13) was calculated to be 11,500 g mol<sup>-1</sup> by end-group analysis of the <sup>1</sup>H NMR spectrum.

Table 2. Synthesis of PCz and PF-containing random copolymers <sup>a</sup>.

Run	Monomers		Random Copolymers	Random Copolymers			Yield <sup>d</sup> (%)
	M <sub>A</sub>	M <sub>B</sub>		$M_{n,SEC}$ <sup>b</sup> (g mol <sup>-1</sup> )	$M_{n,NMR}$ <sup>c</sup> (g mol <sup>-1</sup> )	$D_M$ <sup>b</sup>	
13	M1	M2	2,7-PCz-co-3,6-PCz	7800	11,500	1.49	72.6
14	M1	M5	PF-co-3,6-PCz	9300	12,800	1.38	74.6
15	M2	M5	PF-co-2,7-PCz	7800	12,500	1.48	76.1

<sup>a</sup> Polymerization condition: Atmosphere, Ar; solvent, THF/water (*v/v*) = 10:1; [M<sub>A</sub>+M<sub>B</sub>]<sub>0</sub> = 10 mmol L<sup>-1</sup>; [M<sub>A</sub>]<sub>0</sub>/[M<sub>B</sub>]<sub>0</sub>/[initiator]<sub>0</sub>/[Pd<sub>2</sub>(dba)<sub>3</sub>•CHCl<sub>3</sub>]/[*t*-Bu<sub>3</sub>P]/[K<sub>3</sub>PO<sub>4</sub>] = 15:15:1:0.3:2.2:1.5. <sup>b</sup> Determined by SEC using PSt standards. <sup>c</sup> Determined by <sup>1</sup>H NMR in CDCl<sub>3</sub>.

<sup>d</sup> Isolated yield.



**Scheme 4.** Random copolymerization of M1/M2, M1/M5, and M2/M5.

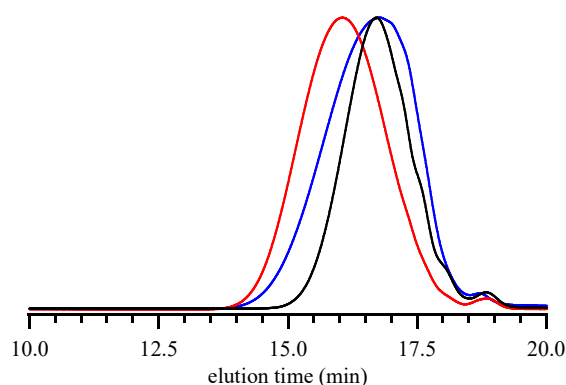


**Figure 9.** SEC traces of 2,7-PCz-co-3,6-PCz (black curve), PF-co-2,7-PCz (red curve), and PF-co-3,6-PCz (blue curve).

In addition, random copolymerization was carried out for the combination of carbazole and fluorene monomers, i.e., M1/M5 and M2/M5 (Scheme 4). Both polymerizations homogeneously proceeded and afforded the corresponding random copolymers, i.e., PF-co-3,6-PCz and PF-co-2,7-PCz, with  $D_M$  values of 1.38 and 1.48, respectively. The  $^1\text{H}$  NMR spectra of the resulted random copolymers showed characteristic signals from both the fluorene and carbazole units (Figure 10), which confirmed the successful synthesis of random copolymers.

The thermal and photophysical properties of 3,6-PCz, 2,7-PCz, and fluorene/carbazole copolymers were investigated (see the supplementary material). Our 3,6-PCz and 2,7-PCz showed thermal and photophysical properties comparable to the reported data [39,40]. The thermal decomposition temperatures of the random copolymers were comparable to those of the constituent polymers. The UV-Vis and fluorescence spectra of the random copolymers were similar to the superposition of the spectra from the constituent homopolymers.

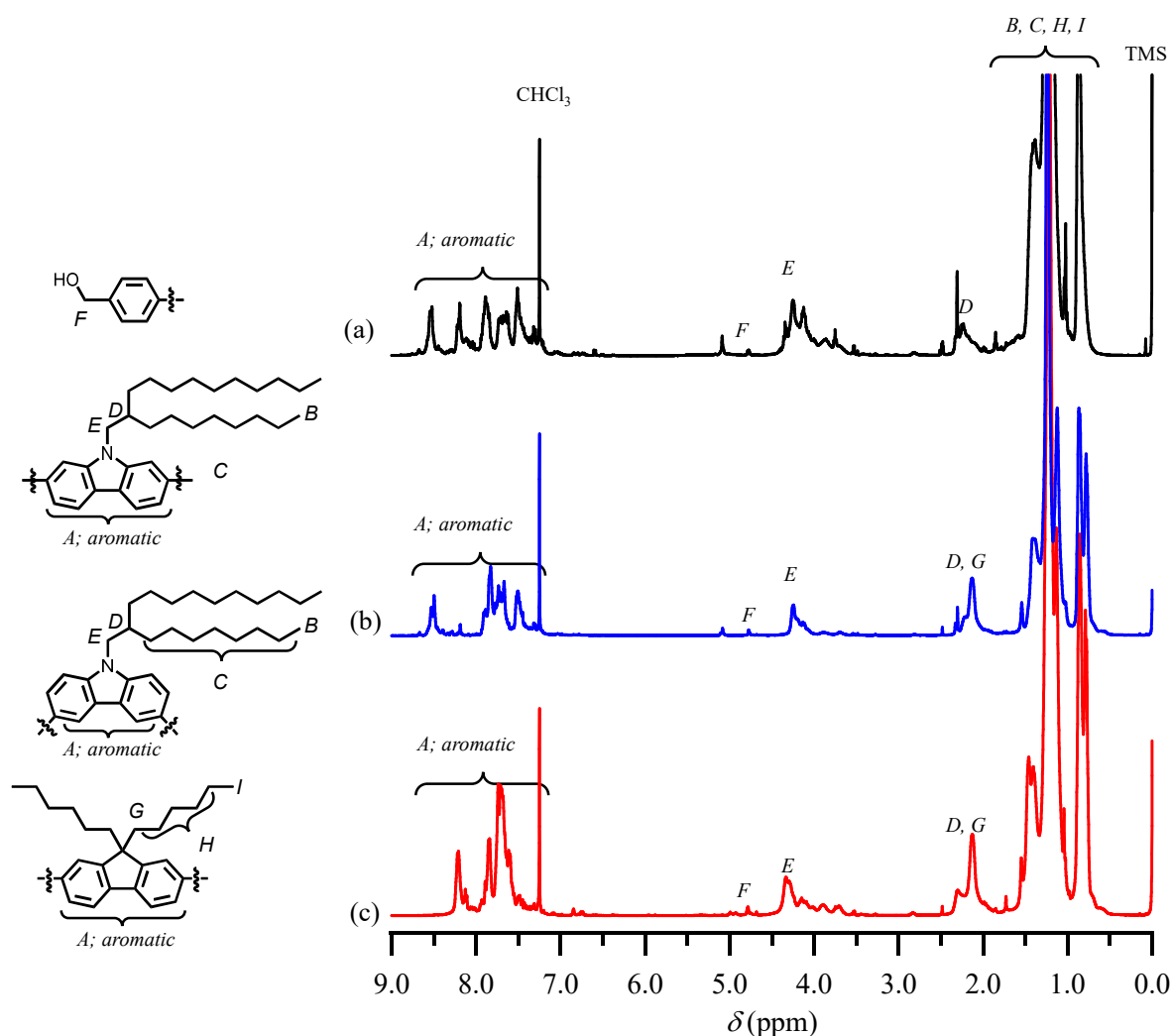
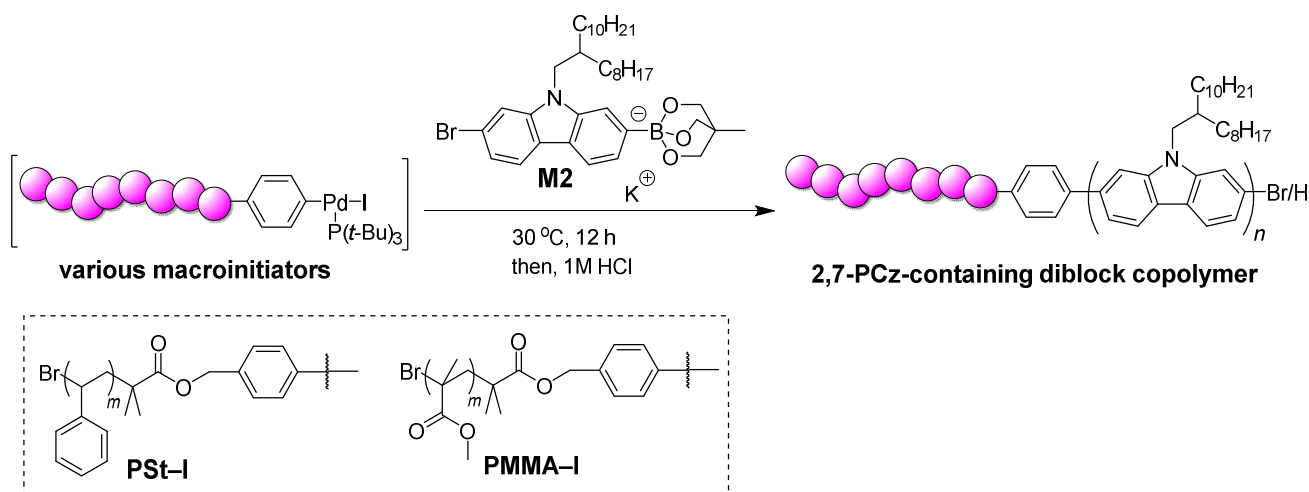


**Figure 10.**  $^1\text{H}$  NMR spectra of (a) 2,7-PCz-co-3,6-PCz, (b) PF-co-3,6-PCz, and (c) PF-co-2,7-PCz (400 MHz,  $\text{CDCl}_3$ ).

#### 3.4. Synthesis of 2,7-PCz-Containing Diblock Copolymers Using Macroinitiators

Finally, we employed iodobenzene-terminated macroinitiators for the SCTP of **M2** in order to synthesize 2,7-PCz-containing block copolymers (Scheme 5). Based on our previous study, we reduced the water content as much as possible to prevent the precipitation of the macroinitiator [49]. We first attempted SCTP with iodobenzene-terminated polystyrene, i.e., PSt-I ( $M_{n,\text{NMR}} = 8300 \text{ g mol}^{-1}$ ,  $D_M = 1.24$ ), as the macroinitiator under the optimized conditions ( $[\text{PSt-I}]_0/[\text{M2}]_0 = 1/15$ ; THF/water ( $v/v$ ) = 5000:1; run 16 in Table 3), giving a PSt-*b*-2,7-PCz diblock copolymer. Importantly, the SEC elution peak clearly shifted toward the shorter retention time, which revealed that **M2** polymerization was initiated from PSt-I (Figure 11). Moreover, the  $^1\text{H}$  NMR spectrum of the resulted product exhibited major signals attributable to both the 2,7-PCz and PSt blocks (Figure 12), confirming the successful synthesis of PSt-*b*-2,7-PCz. The  $M_{n,\text{NMR}}$  of the 2,7-PCz block was calculated to be  $15,500 \text{ g mol}^{-1}$ . In a similar manner, SCTP with the iodobenzene-terminated poly(methyl methacrylate) macroinitiator, i.e., PMMA-I ( $M_{n,\text{NMR}} = 8900 \text{ g mol}^{-1}$ ,  $D_M = 1.09$ ), was conducted (run 17 in Table 3), which afforded PMMA-*b*-2,7-PCz with a  $D_M$  of 1.33 (Figures 11 and 12). These results confirmed the high potential of the present SCTP system for the synthesis of end-functionalized 2,7-PCz and 2,7-PCz-containing block copolymers.



**Scheme 5.** Syntheses of PSt-*b*-2,7-PCz and PMMA-*b*-2,7-PCz by SCTP using PSt-I and PMMA-I macroinitiators, respectively.

**Table 3.** Polymerization of M2 using macroinitiators <sup>a</sup>.

Run	Macroinitiator		Block Copolymer				
		$M_{n,NMR}^c$ (g mol <sup>-1</sup> )	$\mathcal{D}_M^b$		$M_{n,NMR}^c$ (g mol <sup>-1</sup> )	$\mathcal{D}_M^b$	Yield <sup>d</sup> (%)
16	PSt-I	8300	1.24	PSt- <i>b</i> -2,7-PCz	15,500	1.31	78.6
17	PMMA-I	8900	1.09	PMMA- <i>b</i> -2,7-PCz	15,700	1.33	73.5

<sup>a</sup> Polymerization condition: atmosphere, Ar; solvent, THF/water (*v/v*) = 5000:1;  $[M2]_0 = 10$  mmol L<sup>-1</sup>;  $[M2]_0/[macroinitiator]_0/[Pd_2(dba)_3 \bullet CHCl_3]/[t-Bu_3P]/[K_3PO_4] = 15:1:1.2:8.8:1.2$ . <sup>b</sup> Determined by SEC using PSt standards. <sup>c</sup> Determined by <sup>1</sup>H NMR in CDCl<sub>3</sub>. <sup>d</sup> Isolated yield.

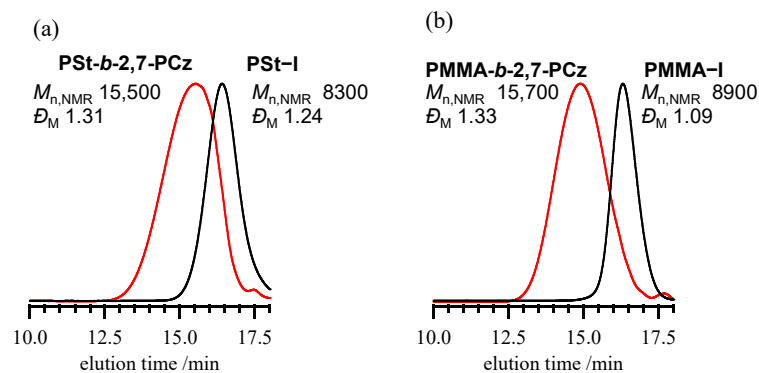


**Figure 11.** SEC traces of (a) PSt-*b*-2,7-PCz and (b) PMMA-*b*-2,7-PCz. The black and red curves represent the macroinitiators and block copolymers, respectively.



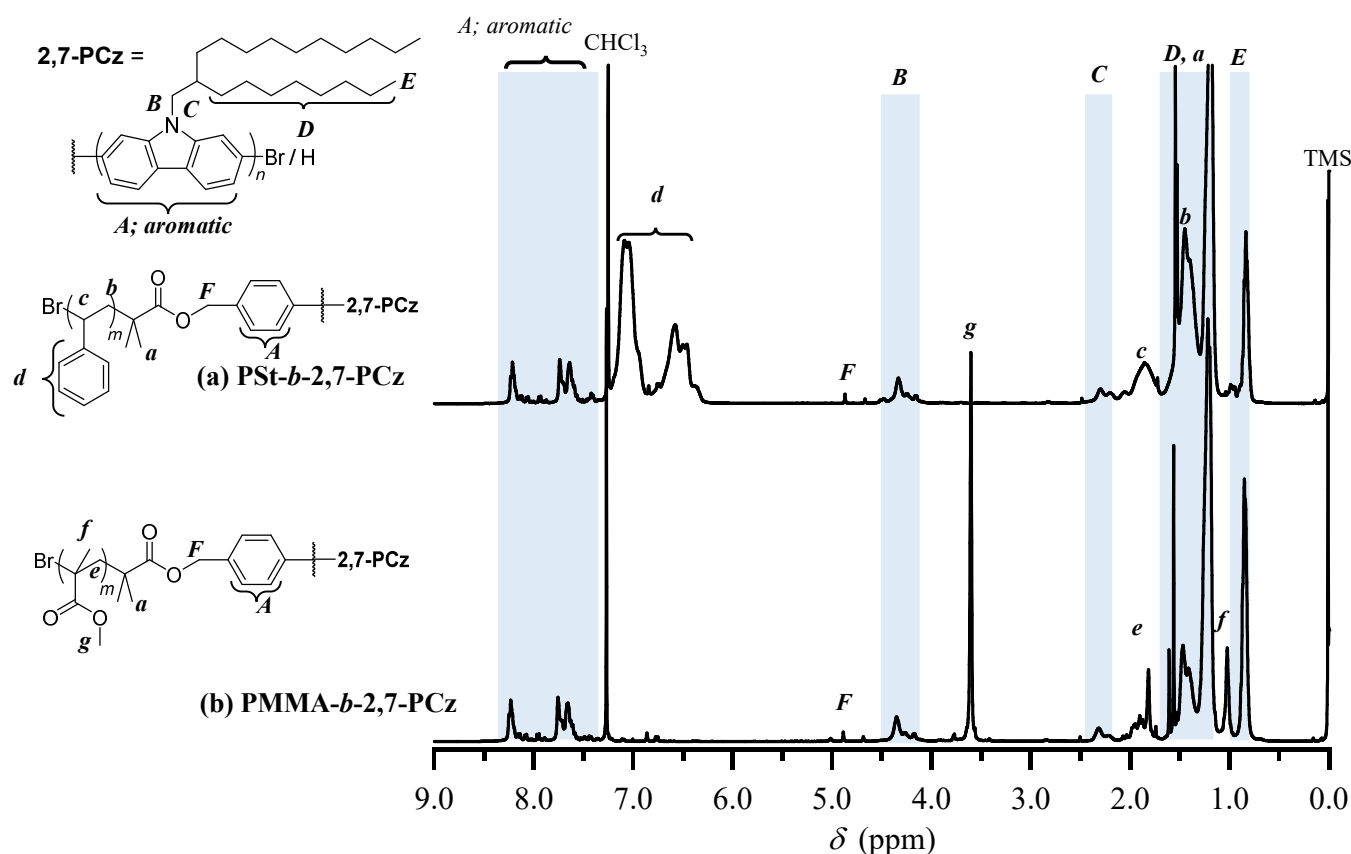


**Figure 12.**  $^1\text{H}$  NMR spectra of (a) PSt-*b*-2,7-PCz and (b) PMMA-*b*-2,7-PCz (400 MHz,  $\text{CDCl}_3$ ).

#### 4. Conclusions

In this study, we investigated the SCTP of triolborate-type carbazole monomers for the first time. The SCTP of potassium 3-(6-bromo-9-(2-octyldodecyl)-9H-carbazole-2-yl)triolborate (M1) at low temperatures selectively produced end-functionalized 3,6-PCz, while suppressing the formation of cyclic by-products. The SCTP of potassium 2-(7-bromo-9-(2-octyldodecyl)-9H-carbazole-2-yl)triolborate (M2) proceeded in a chain-growth mechanism and controlled/living fashion to produce 2,7-PCzs with controlled molecular weights ( $5080\text{--}37,900\text{ g mol}^{-1}$ ) and a relatively narrow  $D_M$  (1.35–1.48). Kinetic and block copolymerization experiments revealed that the SCTP proceeded in chain growth and a controlled/living polymerization manner. Overall, we found that the precise synthesis of 3,6- and 2,7-PCzs can be realized using a triolborate-type monomer with higher nucleophilicity than those of conventionally used pinacolboronate-type monomers. In addition, the present SCTP approach enabled the synthesis of random copolymers of *N*-alkyl-3,6- and 2,7-carbazoles, random copolymers of *N*-alkyl-carbazole and 9,9-dialkylfluorene, and 2,7-PCz-containing block copolymers. We believe that this system provides easy access to a variety of functionalized polycarbazoles, eventually facilitating the development of polycarbazole-based organic devices.

**Supplementary Materials:** The following are available online at <https://www.mdpi.com/article/10.3390/polym13234168/s1>. Experimental section, additional discussion for polymer syntheses, and  $^1\text{H}$  NMR, SEC, and MALDI-TOF MS data for various samples (PDF). Figure S1: (a) SEC trace of 3,6-PCz (run 1, Table 1) detected by RI detector (eluent, THF; flow rate,  $1.0\text{ mL min}^{-1}$ ). (c) MALDI-TOF mass spectrum of 3,6-PCz obtained from run 1 (Table 1). (b and d) SEC trace and MALDI-TOF mass spectrum of 3,6-PCz obtained from run 1 after preparative SEC. Figure S2: Expanded MALDI-TOF mass spectra ranging from 1200 to 4000 Da of 3,6-PCz. Figure S3: SEC traces of crude reaction

mixture for the SCTP of M3 (upper) and M4 (lower) (eluent, THF; flow rate, 1.0 mL min<sup>-1</sup>). Table S1: Monomer conversion, molecular weight, and dispersity at each reaction time.

**Author Contributions:** S.K. conducted the experiments and wrote the manuscript. T.I. and T.S. designed the experiments and assisted in writing the article. M.A., T.Y., K.T. and Y.Y. also contributed by co-authoring the manuscript. All authors have read and agreed to the published version of the manuscript.

**Funding:** This research was funded by the JSPS Grant-in-Aid for Scientific Research (B), (grant number 19H02769), MEXT Grant-in-Aid for Scientific Research on Innovative Areas (Hybrid Catalysis for Enabling Molecular Synthesis on Demand; grant numbers 18H04639 and 20H04798), Frontier Chemistry Center (Hokkaido University), Photo-excitonix Project (Hokkaido University), and Creative Research Institute (CRIS, Hokkaido University).

**Institutional Review Board Statement:** Not applicable.

**Informed Consent Statement:** Not applicable.

**Conflicts of Interest:** The authors declare no conflict of interest.

## References

1. Moliton, A.; Hiorns, R.C. Review of electronic and optical properties of semiconducting  $\pi$ -conjugated polymers: Applications in optoelectronics. *Polym. Int.* **2004**, *53*, 1397–1412. [[CrossRef](#)]
2. Guo, X.; Baumgarten, M.; Müllen, K. Designing  $\pi$ -conjugated polymers for organic electronics. *Prog. Polym. Sci.* **2013**, *38*, 1832–1908. [[CrossRef](#)]
3. Hide, F.; Díaz-García, M.A.; Schwartz, B.J.; Heeger, A.J. New developments in the photonic applications of conjugated polymers. *Acc. Chem. Res.* **1997**, *30*, 430–436. [[CrossRef](#)]
4. Grimsdale, A.C.; Chan, K.L.; Martin, R.E.; Jokisz, P.G.; Holmes, A.B. Synthesis of light-emitting conjugated polymers for applications in electroluminescent devices. *Chem. Rev.* **2009**, *109*, 897–1091. [[PubMed](#)]
5. Kimpel, J.; Michinobu, T. Conjugated polymers for functional applications: Lifetime and performance of polymeric organic semiconductors in organic field-effect transistors. *Polym. Int.* **2021**, *70*, 367–373. [[CrossRef](#)]
6. Yang, J.; Zhao, Z.; Wang, S.; Guo, Y.; Liu, Y. Insight into high-performance conjugated polymers for organic field-effect transistors. *Chem* **2018**, *4*, 2748–2785. [[CrossRef](#)]
7. Cheng, Y.J.; Yang, S.H.; Hsu, C.S. Synthesis of conjugated polymers for organic solar cell applications. *Chem. Rev.* **2009**, *109*, 5868–5923. [[CrossRef](#)]
8. Su, Y.-W.; Lan, S.-C.; Wei, K.-H. Organic photovoltaics. *Mater. Today* **2012**, *12*, 554–563. [[CrossRef](#)]
9. Han, S.T.; Zhou, Y.; Roy, V.A.L. Towards the development of flexible non-volatile memories. *Adv. Mater.* **2013**, *25*, 5425–5449. [[CrossRef](#)]
10. Heremans, P.; Gelinck, G.H.; Müller, R.; Baeg, K.-J.; Kim, D.-Y.; Noh, Y.-Y. Polymer and organic nonvolatile memory devices. *Chem. Mater.* **2010**, *23*, 341–358. [[CrossRef](#)]
11. Hsu, L.C.; Isono, T.; Lin, Y.C.; Kobayashi, S.; Chiang, Y.C.; Jiang, D.H.; Hung, C.C.; Ercan, E.; Yang, W.C.; Hsieh, H.C.; et al. Stretchable OFET memories: Tuning the morphology and the charge-trapping ability of conjugated block copolymers through soft segment branching. *ACS Appl. Mater. Interfaces* **2021**, *13*, 2932–2943. [[CrossRef](#)]
12. Yamamoto, T.; Komarudin, D.; Arai, M.; Lee, B.-L.; Suganuma, H.; Asakawa, N.; Inoue, Y.; Kubota, K.; Sasaki, S.; Fukuda, T.; et al. Extensive studies on  $\pi$ -stacking of poly(3-alkylthiophene-2,5-diyl)s and poly(4-alkylthiazole-2,5-diyl)s by optical spectroscopy, NMR analysis, light scattering analysis, and X-ray crystallography. *J. Am. Chem. Soc.* **1998**, *120*, 2047–2058. [[CrossRef](#)]
13. McCullough, R.D. The chemistry of conducting polythiophenes. *Adv. Mater.* **1998**, *10*, 93–116. [[CrossRef](#)]
14. Han, J.; Zong, L.; Liu, C.; Wang, J.; Jian, X. Nickel-catalysed Kumada polycondensation of di-functionalized Grignard reagent with aryl fluoride. *Polym. Int.* **2016**, *65*, 526–534. [[CrossRef](#)]
15. Tamba, S.; Okubo, Y.; Sugie, A.; Mori, A. Synthesis of  $\pi$ -conjugated poly(thienylenearylene)s with nickel-catalyzed C–H functionalization polycondensation. *Polym. J.* **2012**, *44*, 1209–1213. [[CrossRef](#)]
16. Siddiqui, M.N.; Mansha, M.; Mehmood, U.; Ullah, N.; Al-Betar, A.F.; Al-Saadi, A.A. Synthesis and characterization of functionalized polythiophene for polymer-sensitized solar cell. *Dyes Pigment.* **2017**, *141*, 406–412. [[CrossRef](#)]
17. Rehahn, M.; Schlüter, A.D.; Wegner, G.; Feast, W.J. Soluble poly(para-phenylene)s. 1. Extension of the Yamamoto synthesis to dibromobenzenes substituted with flexible side chains. *Polymer* **1989**, *30*, 1054–1059. [[CrossRef](#)]
18. Yamamoto, T.; Yamamoto, A. A novel type of polycondensation of polyhalogenated organic aromatic compounds producing thermostable polyphenylene type polymers promoted by nickel complexes. *Chem. Lett.* **1977**, *6*, 353–356. [[CrossRef](#)]
19. Chen, L.; Wang, K.; Mahmoud, S.M.; Li, Y.; Huang, H.; Huang, W.; Xu, J.; Dun, C.; Carroll, D.; Pietrangelo, A. Effects of replacing thiophene with 5,5-dimethylcyclopentadiene in alternating poly(phenylene), poly(3-hexylthiophene), and poly(flourene) copolymer derivatives. *Polym. Chem.* **2015**, *6*, 7533–7542. [[CrossRef](#)]

20. Ranger, M.; Rondeau, D.; Leclerc, M. New well-defined poly(2,7-fluorene) derivatives: Photoluminescence and base doping. *Macromolecules* **1997**, *30*, 7686–7691. [[CrossRef](#)]
21. Zheng, M.; Ding, L.; Lin, Z.; Karasz, F.E. Synthesis and characterization of fluorenediylvinylene and thiophenediylvinylene-containing terphenylene-based copolymers. *Macromolecules* **2002**, *35*, 9939–9946. [[CrossRef](#)]
22. Lightowler, S.; Hird, M. Palladium-catalyzed cross-coupling reactions in the synthesis of novel aromatic polymers. *Chem. Mater.* **2004**, *16*, 3963–3971. [[CrossRef](#)]
23. Yuan, C.; Fang, Q. A new procedure for the synthesis of  $\pi$ -conjugated polymers via ligand-free iron(iii)-catalyzed oxidative homocoupling reaction of Grignard reagents. *RSC Adv.* **2012**, *2*, 8055–8060. [[CrossRef](#)]
24. Loewe, R.S.; Ewbank, P.C.; Liu, J.; Zhai, L.; McCullough, R.D. Regioregular, head-to-tail coupled poly(3-alkylthiophenes) made easy by the GRIM method: Investigation of the reaction and the origin of regioselectivity. *Macromolecules* **2001**, *34*, 4324–4333. [[CrossRef](#)]
25. Miyakoshi, R.; Yokoyama, A.; Yokozawa, T. Catalyst-transfer polycondensation. Mechanism of Ni-catalyzed chain-growth polymerization leading to well-defined poly(3-hexylthiophene). *J. Am. Chem. Soc.* **2005**, *127*, 17542–17547. [[CrossRef](#)]
26. Yokoyama, A.; Suzuki, H.; Kubota, Y.; Ohuchi, K.; Higashimura, H.; Yokozawa, T. Chain-growth polymerization for the synthesis of polyfluorene via Suzuki-Miyaura coupling reaction from an externally added initiator unit. *J. Am. Chem. Soc.* **2007**, *129*, 7236–7237. [[CrossRef](#)]
27. Morin, J.-F.; Leclerc, M.; Adés, D.; Siove, A. Polycarbazoles: 25 years of progress. *Macromol. Rapid Commun.* **2005**, *26*, 761–778. [[CrossRef](#)]
28. Xu, F.; Kim, J.-H.; Kim, H.U.; Jang, J.-H.; Yook, K.S.; Lee, J.Y.; Hwang, D.-H. Synthesis of high-triplet-energy host polymer for blue and white electrophosphorescent light-emitting diodes. *Macromolecules* **2014**, *47*, 7397–7406. [[CrossRef](#)]
29. Huang, J.; Niu, Y.H.; Yang, W.; Mo, Y.Q.; Yuan, M.; Cao, Y. Novel electroluminescent polymers derived from carbazole and benzothiadiazole. *Macromolecules* **2002**, *35*, 6080–6082. [[CrossRef](#)]
30. Li, Z.A.; Liu, Y.; Yu, G.; Wen, Y.; Guo, Y.; Ji, L.; Qin, J.; Li, Z. A new carbazole-constructed hyperbranched polymer: Convenient one-pot synthesis, hole-transporting ability, and field-effect transistor properties. *Adv. Funct. Mater.* **2009**, *19*, 2677–2683. [[CrossRef](#)]
31. Liu, S.-J.; Lin, W.-P.; Yi, M.-D.; Xu, W.-J.; Tang, C.; Zhao, Q.; Ye, S.-H.; Liu, X.-M.; Huang, W. Conjugated polymers with cationic iridium (iii) complexes in the side-chain for flash memory devices utilizing switchable through-space charge transfer. *J. Mater. Chem.* **2012**, *22*, 22964–22970. [[CrossRef](#)]
32. Luo, J.; Xie, G.; Gong, S.; Chen, T.; Yang, C. Creating a thermally activated delayed fluorescence channel in a single polymer system to enhance exciton utilization efficiency for bluish-green electroluminescence. *Chem. Commun.* **2016**, *52*, 2292–2295. [[CrossRef](#)]
33. Michinobu, T.; Kumazawa, H.; Otsuki, E.; Usui, H.; Shigehara, K. Synthesis and properties of nitrogen-linked poly(2,7-carbazole)s as hole-transport material for organic light emitting diodes. *J. Polym. Sci. A Polym. Chem.* **2009**, *47*, 3880–3891. [[CrossRef](#)]
34. Yi, L.; Wang, X. Theoretical investigation of nitrogen-linked poly(2,7-carbazole)s as hole-transport materials for organic light emitting diodes. *Comp. Theor. Chem.* **2011**, *969*, 71–75. [[CrossRef](#)]
35. Peng, F.; Wang, X.; Guo, T.; Xiong, J.; Ying, L.; Cao, Y. Realizing efficient bipolar deep-blue light-emitting poly(2,7-carbazole) derivatives by suppressing intramolecular charge transfer. *Organic* **2019**, *67*, 34–42. [[CrossRef](#)]
36. Li, J.; Dierschke, F.; Wu, J.; Grimsdale, A.C.; Müllen, K. Poly(2,7-carbazole) and perylene tetracarboxydiimide: A promising donor/acceptor pair for polymer solar cells. *J. Mater. Chem.* **2006**, *16*, 96–100. [[CrossRef](#)]
37. Blouin, N.; Leclerc, M. Poly(2,7-carbazole)s: Structure-property relationships. *Acc. Chem. Res.* **2008**, *41*, 1110–1119. [[CrossRef](#)]
38. Wakim, S.; Beaupré, S.; Blouin, N.; Aich, B.; Rodman, S.; Gaudiana, R.; Tao, Y.; Leclerc, M. Highly efficient organic solar cells based on a poly(2,7-carbazole) derivative. *J. Mater. Chem.* **2009**, *19*, 5351–5358. [[CrossRef](#)]
39. Morin, J.-F.; Leclerc, M. Syntheses of conjugated polymers derived from *N*-alkyl-2,7-carbazoles. *Macromolecules* **2001**, *34*, 4680–4682. [[CrossRef](#)]
40. Zhang, Z.-B.; Fujiki, M.; Tang, H.-Z.; Motonaga, M.; Torimitsu, K. The first high molecular weight poly(*N*-alkyl-3,6-carbazole)s. *Macromolecules* **2002**, *35*, 1988–1990. [[CrossRef](#)]
41. Schroot, R.; Schubert, U.S.; Jäger, M. Poly(*N*-alkyl-3,6-carbazole)s via Kumada catalyst transfer polymerization: Impact of metal-halogen exchange. *Macromolecules* **2016**, *49*, 8801–8811. [[CrossRef](#)]
42. Wen, H.; Ge, Z.; Liu, Y.; Yokozawa, T.; Lu, L.; Ouyang, X.; Tan, Z. Efficient synthesis of well-defined polycarbazoles via catalyst-transfer Kumada coupling polymerization. *Eur. Polym. J.* **2013**, *49*, 3740–3743. [[CrossRef](#)]
43. Schroot, R.; Schubert, U.S.; Jäger, M. Poly(*N*-alkyl-3,6-carbazole)s via Suzuki-Miyaura polymerization: From macrocyclization toward end functionalization. *Macromolecules* **2017**, *50*, 1319–1330. [[CrossRef](#)]
44. Brown, H.C.; Zaidlewicz, M. *Organic Synthesis via Boranes*; Aldrich: Milwaukee, WI, USA, 2001; Volume 2.
45. Miyaura, N.; Suzuki, A. Palladium-catalyzed cross-coupling reactions of organoboron compounds. *Chem. Rev.* **1995**, *95*, 2457–2483. [[CrossRef](#)]
46. Yamamoto, Y.; Takizawa, M.; Yu, X.-Q.; Miyaura, N. Cyclic triolborates: Air- and water-stable ate complexes of organoboronic acids. *Angew. Chem. Int. Ed.* **2008**, *47*, 928–931. [[CrossRef](#)]
47. Li, G.-Q.; Yamamoto, Y.; Miyaura, N. Double-coupling of dibromo arenes with aryltriolborates for synthesis of diaryl-substituted planar frameworks. *Tetrahedron* **2011**, *67*, 6804–6811. [[CrossRef](#)]

48. Sakashita, S.; Takizawa, M.; Sugai, J.; Ito, H.; Yamamoto, Y. Tetrabutylammonium 2-pyridyltriolborate salts for Suzuki-Miyaura cross-coupling reactions with aryl chlorides. *Org. Lett.* **2013**, *15*, 4308–4311. [[CrossRef](#)]
49. Kobayashi, S.; Fujiwara, K.; Jiang, D.; Yamamoto, T.; Tajima, K.; Yamamoto, Y.; Isono, T.; Satoh, T. Suzuki–Miyaura catalyst-transfer polycondensation of triolborate-type fluorene monomer: Toward rapid access to polyfluorene-containing block and graft copolymers from various macroinitiators. *Polym. Chem.* **2020**, *11*, 6832–6839. [[CrossRef](#)]
50. Zhang, H.-H.; Xing, C.-H.; Hu, Q.-S.; Hong, K. Controlled Pd(0)/ *t*-Bu<sub>3</sub>P-catalyzed Suzuki cross-coupling polymerization of AB-type monomers with ArPd(*t*-Bu<sub>3</sub>P)X or Pd<sub>2</sub>(dba)<sub>3</sub>/*t*-Bu<sub>3</sub>P/ArX as the initiator. *Macromolecules* **2015**, *48*, 967–978. [[CrossRef](#)]
51. Lee, J.; Park, H.; Hwang, S.-H.; Lee, I.-H.; Choi, T.-L. RuPhos Pd precatalyst and MIDA boronate as an effective combination for the precision synthesis of poly(3-hexylthiophene): Systematic investigation of the effects of boronates, halides, and ligands. *Macromolecules* **2020**, *53*, 3306–3314. [[CrossRef](#)]
52. Beryozkina, T.; Senkovskyy, V.; Kaul, E.; Kiriya, A. Kumada catalyst-transfer polycondensation of thiophene-based oligomers: Robustness of a chain-growth mechanism. *Macromolecules* **2008**, *41*, 7817–7823. [[CrossRef](#)]
53. Doubina, N.; Ho, A.; Jen, A.K.-Y.; Luscombe, C.K. Effect of initiators on the Kumada catalyst-transfer polycondensation reaction. *Macromolecules* **2009**, *42*, 7670–7677. [[CrossRef](#)]
54. Marshall, N.; Sontag, S.K.; Locklin, J. Substituted poly(*p*-phenylene) thin films via surface-initiated kumada-type catalyst transfer polycondensation. *Macromolecules* **2010**, *43*, 2137–2144. [[CrossRef](#)]
55. Adamo, C.; Amatore, C.; Ciofini, I.; Jutand, A.; Lakmini, H. Mechanism of the palladium-catalyzed homocoupling of arylboronic acids: Key involvement of a palladium peroxo complex. *J. Am. Chem. Soc.* **2006**, *128*, 6829–6836. [[CrossRef](#)] [[PubMed](#)]
56. Butters, M.; Harvey, J.N.; Jover, J.; Lennox, A.J.J.; Lloyd-Jones, G.C.L.; Murray, P.M. Aryl trifluoroborates in Suzuki-Miyaura coupling: The roles of endogenous aryl boronic acid and fluoride. *Angew. Chem.* **2010**, *122*, 5282–5286. [[CrossRef](#)]
57. Lemasson, F.; Berton, N.; Tittmann, J.; Hennrich, F.; Kappes, M.M.; Mayor, M. Polymer library comprising fluorene and carbazole homo- and copolymers for selective single-walled carbon nanotubes extraction. *Macromolecules* **2012**, *45*, 713–722. [[CrossRef](#)]